Vesicle dynamics in Newtonian and non-Newtonian fluids

Ming-Chih Lai
mclai@math.nctu.edu.tw

Department of Applied Mathematics
National Chiao Tung University
Taiwan

Modelling and Simulation of Interface Dynamics in Fluids/Solids and Applications, 14-18, May 2018

Vesice problem: Navier-Stokes + surface dynamics with PDE constraint

- Vesicle can be visualized as a bubble of liquid within another liquid with a closed lipid membrane suspended in aqueous solution, size is about $10\mu m$
- Lipid membrane consists of tightly packed lipid molecules with hydrophilic heads facing the exterior and interior fluids and hydrophobic tails hiding in the middle, thickness is about $6nm$ so we treat the membrane as a surface (3d) or a curve (2d)
- Lipid membrane (or vesicle boundary) can deform but resist area dilation, that is surface incompressible

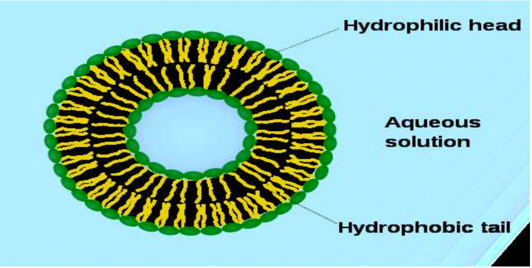

Questions: How the vesicle behaves in fluid flows?

- To mimic some mechanical behavior of red blood cells (RBC), drug carrying capsules in capillary
- In shear flow: Tank-treading (TT), Tumbling (TU), Trembling (TR), depend on the viscosity contrast $\lambda = \mu_{in}/\mu_{out}$; Keller & Skalak JFM, 1982 (theory), Deschamps et. al. PNAS, 2009 (experiment)
- Amoeboid motion (active vesicle swimmer) in confined geometry, Wu et. al. Lai & Misbah, PRE-Rapid 2015, Soft Matter 2016

Figure: Red blood cells: flexible biconcave disks

Numerical simulation: single vesicle in a shear flow

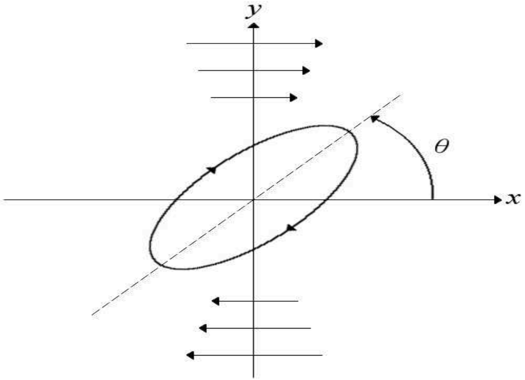

Figure: Inclination angle and tank-treading in a simple shear flow

Tank-treading to tumbling transitions, Kim & Lai, PRE 2012

Different viscosity effect

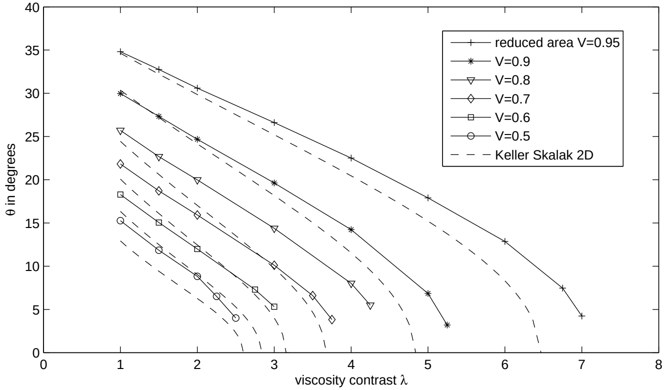

Figure: The inclination angle θ versus the viscosity contrast $\lambda = \frac{\mu_{in}}{\mu_{out}}$. The simulation results (solid lines) are compared with the Keller & Skallak theory (dashed lines).

Immersed boundary (IB) and immersed interface (IIM) methods for vesicle dynamics

- Simulating the dynamics of 2D inextensible vesicles by the penalty immersed boundary method (Kim & Lai JCP 2010), inertial effect (Kim & Lai PRE 2012), 2D 4-roll mill flows (Kim, Lai & Seol PRE 2017)
- Nearly inextensible approach (3D axisymmetric case, Hu, Kim & Lai JCP 2014, Full 3D case, Seol, Hu, Kim & Lai JCP 2016)
- IIM for inextensible interfaces in Navier-Stokes flow (Li & Lai, EAJAM, 2011)
- A fractional step immersed boundary method for Stokes flow with an inextensible interface enclosing a solid particle (SISC 2012)
- Unconditionally energy stable penalty IB method without bending (Hu & Lai EAJAM 2013, Hsieh, Lai, Yang & You JSC 2015)
- Vesicle electrohydroynamics using IB and IIM (Hu, Lai, Seol & Young, JCP 2016)
- Amoeboid swimming (Misbah and Lai et. PRE 2015, Soft matter 2016)

Mathematical modeling on vesicle problem

- Vesicle: A liquid drop within another liquid with a closed lipid membrane
- Vesicle boundary Σ: represented by $\mathbf{X}$, is able to deform, but resist area dilation, i.e. Σ is surface incompressible (or inextensible)
- The fluid-structure interaction is formulated by the stress balance condition on Σ

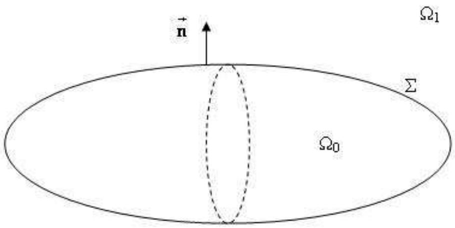

Immersed Boundary (IB) formulation: treat the vesicle boundary as a force generator

$$\begin{aligned}
\rho\left(\frac{\partial \boldsymbol{u}}{\partial t} + \boldsymbol{u}\cdot\nabla\boldsymbol{u}\right) + \nabla p &= \mu\Delta\boldsymbol{u} + \boldsymbol{f} \qquad \text{in } \Omega \\
\nabla\cdot\boldsymbol{u} &= 0 \qquad \text{in } \Omega \\
\nabla_s\cdot\boldsymbol{U} &= 0 \qquad \text{on } \Sigma \\
\frac{\partial \mathbf{X}}{\partial t} &= \boldsymbol{U} = \int_\Omega \mathbf{u}(\mathbf{x},t)\delta(\mathbf{x}-\mathbf{X})d\mathbf{x}
\end{aligned}$$

where the immersed boundary force

$$\begin{aligned}
\boldsymbol{f} &= \int_\Sigma \boldsymbol{F}(\boldsymbol{X})\,\delta(\boldsymbol{x}-\boldsymbol{X})\;d\boldsymbol{X} \\
\boldsymbol{F} &= \boldsymbol{F}_b + \boldsymbol{F}_\sigma \qquad \text{on } \Sigma \\
\boldsymbol{F}_b &= \frac{c_b}{2}\left(\Delta_s H + 2H(H^2-K)\right)\boldsymbol{n} \\
\boldsymbol{F}_\sigma &= \nabla_s\sigma - 2\,H\,\sigma\boldsymbol{n}
\end{aligned}$$

- H: mean curvature, K: Gaussian curvature,

$$\nabla_s = \nabla - \frac{\partial}{\partial \boldsymbol{n}}\boldsymbol{n}, \qquad \Delta_s = \nabla_s \cdot \nabla_s$$

- c_b: bending rigidity
- σ: unknown elastic tension to be introduced to enforce $\nabla_s \cdot \boldsymbol{U} = 0$
- It can be shown that the tension doesn't do extra work to the fluid; i.e. $< S(\sigma), \mathbf{u} >_\Omega = - < \sigma, \nabla_s \cdot \boldsymbol{U} >_\Sigma$
- The pressure and elastic tension have the same roles as Lagrange multipliers

Question: Where does the boundary force $\boldsymbol{F}$ come from?

Answer: Variational derivative of Helfrich energy

$$\begin{aligned} E &= \frac{c_b}{2}\int_\Sigma H^2 \, d\boldsymbol{S} + \int_\Sigma \sigma \, d\boldsymbol{S} \\ \Rightarrow \boldsymbol{F} &= -\frac{\delta E}{\delta \boldsymbol{X}} = \boldsymbol{F}_b + \boldsymbol{F}_\sigma \end{aligned}$$

Basic surface geometry

For the vesicle surface $\mathbf{X}(r,s)$, the first fundamental forms

$$E = \mathbf{X}_r \cdot \mathbf{X}_r, \quad F = \mathbf{X}_r \cdot \mathbf{X}_s, \quad \text{and} \quad G = \mathbf{X}_s \cdot \mathbf{X}_s,$$

then

- $\nabla_s \sigma = \dfrac{G\mathbf{X}_r - F\mathbf{X}_s}{EG - F^2}\sigma_r + \dfrac{E\mathbf{X}_s - F\mathbf{X}_r}{EG - F^2}\sigma_s$
- $\nabla_s \cdot \mathbf{U} = \dfrac{G\mathbf{X}_r - F\mathbf{X}_s}{EG - F^2} \cdot \mathbf{U}_r + \dfrac{E\mathbf{X}_s - F\mathbf{X}_r}{EG - F^2} \cdot \mathbf{U}_s$
- Using $\mathbf{a} \times (\mathbf{b} \times \mathbf{c}) = (\mathbf{a} \cdot \mathbf{c})\mathbf{b} - (\mathbf{a} \cdot \mathbf{b})\mathbf{c}$,
  we obtain two useful relations

$$\mathbf{X}_s \times \mathbf{n} = \frac{G\mathbf{X}_r - F\mathbf{X}_s}{|\mathbf{X}_r \times \mathbf{X}_s|}, \quad \mathbf{n} \times \mathbf{X}_r = \frac{E\mathbf{X}_s - F\mathbf{X}_r}{|\mathbf{X}_r \times \mathbf{X}_s|}$$

which give

- $\nabla_s \sigma = \dfrac{(\mathbf{X}_s \times \mathbf{n})\sigma_r + (\mathbf{n} \times \mathbf{X}_r)\sigma_s}{|\mathbf{X}_r \times \mathbf{X}_s|}$ and
- $\nabla_s \cdot \mathbf{U} = \dfrac{(\mathbf{X}_s \times \mathbf{n}) \cdot \mathbf{U}_r + (\mathbf{n} \times \mathbf{X}_r) \cdot \mathbf{U}_s}{|\mathbf{X}_r \times \mathbf{X}_s|}$

More useful identities

- $$(\mathbf{X}_s \times \mathbf{n})\sigma_r + (\mathbf{n} \times \mathbf{X}_r)\sigma_s = \nabla_s \sigma \, |\mathbf{X}_r \times \mathbf{X}_s|$$
- $$(\mathbf{X}_s \times \mathbf{n}) \cdot \mathbf{U}_r + (\mathbf{n} \times \mathbf{X}_r) \cdot \mathbf{U}_s = \nabla_s \cdot \mathbf{U} \, |\mathbf{X}_r \times \mathbf{X}_s|$$
- $$\mathbf{X}_s \times \mathbf{n}_r + \mathbf{n}_s \times \mathbf{X}_r = -2H\mathbf{n} \, |\mathbf{X}_r \times \mathbf{X}_s|$$
- $$(\mathbf{X}_s \times \mathbf{n})_r + (\mathbf{n} \times \mathbf{X}_r)_s = -2H\mathbf{n} \, |\mathbf{X}_r \times \mathbf{X}_s|$$
- $$\left(\sigma(\mathbf{X}_s \times \mathbf{n})\right)_r + \left(\sigma(\mathbf{n} \times \mathbf{X}_r)\right)_s = (\nabla_s \sigma - 2\sigma H \mathbf{n}) \, |\mathbf{X}_r \times \mathbf{X}_s|$$

Relations to Geometric PDEs

Motion by mean curvature

- Motion by mean curvature: $\frac{d\mathbf{X}}{dt} = -\frac{\delta E_\sigma}{\delta \mathbf{X}} = \mathbf{F}_\sigma = -\sigma 2H\mathbf{n}$, σ is a constant, L^2 gradient flow, a convex surface shrinks

Willmore flow

- Willmore energy $E_b(\mathbf{X}) = \frac{c_b}{2}\int_\Sigma H^2 dS$, in physics terminology, surface bending energy (membrane lipid bilayer exhibits a bending resistance)
- In some literature, use $2H$ instead of H
- Willmore flow: $\frac{d\mathbf{X}}{dt} = -\frac{\delta E_b}{\delta \mathbf{X}} = \mathbf{F}_b = \frac{c_b}{2}(\Delta_s H + 2H(H^2 - K))\mathbf{n}$, L^2 gradient flow

Why does $\nabla_s \cdot \boldsymbol{U} = 0$ mean the surface incompressibility?

$$
\begin{aligned}
\frac{\partial}{\partial t}|\mathbf{X}_r \times \mathbf{X}_s| &= \frac{\mathbf{X}_r \times \mathbf{X}_s}{|\mathbf{X}_r \times \mathbf{X}_s|} \cdot (\mathbf{X}_{rt} \times \mathbf{X}_s + \mathbf{X}_r \times \mathbf{X}_{st}) \\
&= \mathbf{n} \cdot (\mathbf{X}_{rt} \times \mathbf{X}_s) + \mathbf{n} \cdot (\mathbf{X}_r \times \mathbf{X}_{st}) \quad \left(\text{since } \mathbf{n} = \tfrac{\mathbf{X}_r \times \mathbf{X}_s}{|\mathbf{X}_r \times \mathbf{X}_s|}\right) \\
&= (\mathbf{X}_s \times \mathbf{n}) \cdot \mathbf{X}_{rt} + (\mathbf{n} \times \mathbf{X}_r) \cdot \mathbf{X}_{st} \quad (\text{using } (\mathbf{a} \times \mathbf{b}) \cdot \mathbf{c} = (\mathbf{b} \times \mathbf{c}) \cdot \mathbf{a}) \\
&= (\mathbf{X}_s \times \mathbf{n}) \cdot \mathbf{U}_r + (\mathbf{n} \times \mathbf{X}_r) \cdot \mathbf{U}_s \quad (\text{since } \mathbf{X}_t = \mathbf{U}) \\
&= \frac{G\mathbf{X}_r - F\mathbf{X}_s}{|\mathbf{X}_r \times \mathbf{X}_s|} \cdot \mathbf{U}_r + \frac{E\mathbf{X}_s - F\mathbf{X}_r}{|\mathbf{X}_r \times \mathbf{X}_s|} \cdot \mathbf{U}_s \quad (\text{using the two relations}) \\
&= (\nabla_s \cdot \mathbf{U})|\mathbf{X}_r \times \mathbf{X}_s| \quad (\text{by the definition of } \nabla_s \cdot \mathbf{U})
\end{aligned}
$$

Skew-adjoint operators, Lai & Seol, AML 2017

$$\langle \mathbf{u}, \mathbf{v} \rangle_\Omega = \int_\Omega \mathbf{u}(\mathbf{x}) \cdot \mathbf{v}(\mathbf{x})\, d\mathbf{x},$$
$$\langle f, g \rangle_\Sigma = \int_\Sigma f(S)\, g(S)\, \mathrm{d}S,$$

Define $S(\sigma) = \int_\Sigma (\nabla_s \sigma - 2\sigma H \mathbf{n}) \delta(\mathbf{x} - \mathbf{X}(r,s,t))\, |\mathbf{X}_r \times \mathbf{X}_s|\; dr\, ds$, then

$$\begin{aligned}
& \langle S(\sigma), \mathbf{u} \rangle_\Omega \\
= & \int_\Omega \left[\int_\Sigma (\nabla_s \sigma - 2\sigma H \mathbf{n})\, |\mathbf{X}_r \times \mathbf{X}_s|\, \delta(\mathbf{x} - \mathbf{X}(r,s,t))\, dr\, ds \right] \cdot \mathbf{u}(\mathbf{x})\, d\mathbf{x} \\
= & \int_\Sigma (\nabla_s \sigma - 2\sigma H \mathbf{n}) \cdot \mathbf{U}(r,s,t)\, |\mathbf{X}_r \times \mathbf{X}_s|\; dr\, ds \\
= & \int_\Sigma (\sigma(\mathbf{X}_s \times \mathbf{n}))_r \cdot \mathbf{U} + (\sigma(\mathbf{n} \times \mathbf{X}_r))_s \cdot \mathbf{U}\, dr ds \\
= & -\int_\Sigma \sigma(\mathbf{X}_s \times \mathbf{n}) \cdot \mathbf{U}_r + \sigma(\mathbf{n} \times \mathbf{X}_r) \cdot \mathbf{U}_s\, dr\, ds \\
= & -\int_\Sigma \sigma(\nabla_s \cdot \mathbf{U})\, |\mathbf{X}_r \times \mathbf{X}_s|\; dr\, ds = -\langle \sigma, \nabla_s \cdot \mathbf{U} \rangle_\Sigma
\end{aligned}$$

Remark: Tension does not do extra work to the fluid. Similar to the pressure in incompressible fluid!

Numerical issues for 3D problem:

1. Coupled with fluid dynamics which vesicle boundary is moving with fluid and whose shape is not known *a priori*
2. Both the volume and the surface area of the vesicle are conserved. How to maintain fluid and vesicle boundary incompressible simultaneously?
3. Need to find H, $\Delta_s H$, $\boldsymbol{n}$, K on a moving surface Σ
4. In additional to the fluid incompressibility, we need extra constraint (surface incompressibility) on the surface
5. The role of pressure p on fluid equations is the same as the role of tension σ on $\nabla_s \cdot \boldsymbol{U} = 0$. Both conditions are local!
6. How to solve the above governing equations efficiently?
7. Boundary integral method, Immersed boundary (Front-tracking), Level-set, Phase field method, Parametric finite element method?

Nearly surface incompressibility approach

- $\nabla_s \cdot \mathbf{U} = 0$ means that $\frac{\partial}{\partial t}|\mathbf{X}_r \times \mathbf{X}_s| = 0$
- To avoid solving the extra unknown tension $\sigma(r, s, t)$, we alternatively use a spring-like elastic tension

$$\sigma = \sigma_0 \left(|\mathbf{X}_r \times \mathbf{X}_s| - |\mathbf{X}_r^0 \times \mathbf{X}_s^0| \right)$$

  where $\sigma_0 \gg 1$ and $|\mathbf{X}_r^0 \times \mathbf{X}_s^0|$ is the initial surface dilating factor
- Similar idea has been used in level set framework by Maitre, Misbah, Peyla & Raoult, Physica D 2012
- The modified elastic energy by

$$E_\sigma(\mathbf{X}) = \frac{\sigma_0}{2} \iint \left(|\mathbf{X}_r \times \mathbf{X}_s| - |\mathbf{X}_r^0 \times \mathbf{X}_s^0| \right)^2 \, drds$$

Derivation of modified elastic force by variational derivative

$$
\begin{aligned}
&\frac{d}{d\varepsilon} E_\sigma(\mathbf{X} + \varepsilon \mathbf{Y})\Big|_{\varepsilon=0} \\
&= \iint \sigma_0 \left(|\mathbf{X}_r \times \mathbf{X}_s| - |\mathbf{X}_r^0 \times \mathbf{X}_s^0| \right) \frac{\mathbf{X}_r \times \mathbf{X}_s}{|\mathbf{X}_r \times \mathbf{X}_s|} \cdot (\mathbf{Y}_r \times \mathbf{X}_s + \mathbf{X}_r \times \mathbf{Y}_s)\, drds \\
&= \iint \sigma \mathbf{n} \cdot (\mathbf{Y}_r \times \mathbf{X}_s + \mathbf{X}_r \times \mathbf{Y}_s)\, drds \quad \left(\text{by } \mathbf{n} = \tfrac{\mathbf{X}_r \times \mathbf{X}_s}{|\mathbf{X}_r \times \mathbf{X}_s|} \right) \\
&= \iint \sigma (\mathbf{X}_s \times \mathbf{n}) \cdot \mathbf{Y}_r + \sigma (\mathbf{n} \times \mathbf{X}_r) \cdot \mathbf{Y}_s\, drds \quad (\text{by the scalar triple product formula}) \\
&= -\iint (\sigma \mathbf{X}_s \times \mathbf{n})_r \cdot \mathbf{Y} + (\sigma \mathbf{n} \times \mathbf{X}_r)_s \cdot \mathbf{Y}\, drds \quad (\text{by integration by parts}) \\
&= -\iint [\sigma_r \mathbf{X}_s \times \mathbf{n} + \sigma_s \mathbf{n} \times \mathbf{X}_r + \sigma (\mathbf{X}_s \times \mathbf{n})_r + \sigma (\mathbf{n} \times \mathbf{X}_r)_s] \cdot \mathbf{Y}\, drds \\
&= -\iint (\sigma_r \mathbf{X}_s \times \mathbf{n} + \sigma_s \mathbf{n} \times \mathbf{X}_r + \sigma \mathbf{X}_s \times \mathbf{n}_r + \sigma \mathbf{n}_s \times \mathbf{X}_r) \cdot \mathbf{Y}\, drds \\
&= -\iint (\nabla_s \sigma - 2\sigma H \mathbf{n}) \cdot \mathbf{Y}\, |\mathbf{X}_r \times \mathbf{X}_s|\, drds \\
&= -\int_\Sigma (\nabla_s \sigma - 2\sigma H \mathbf{n}) \cdot \mathbf{Y}\, \mathrm{d}S \quad (\text{since } \mathrm{d}S = |\mathbf{X}_r \times \mathbf{X}_s|\, drds) \\
&= -\int_\Sigma \mathbf{F}_\sigma \cdot \mathbf{Y}\, \mathrm{d}S
\end{aligned}
$$

$\mathbf{F}_\sigma$ are exactly identical !

Numerical algorithm: axis-symmetric case, Hu, Kim & Lai, JCP 2014

1. Compute the vesicle boundary force

$$\sigma^n = \sigma_0 \left(R^n \left| \mathbf{X}_s \right|^n - R^0 \left| \mathbf{X}_s \right|^0 \right), \quad \mathbf{F}_\sigma^n = \sigma_s^n \boldsymbol{\tau}^n + \sigma^n \boldsymbol{\tau}_s^n - \frac{Z_s^n}{R^n} \sigma^n \mathbf{n}^n,$$

$$\mathbf{F}_b^n = c_b(\Delta_s H^n + 2H^n((H^n)^2 - K^n)) \left| \mathbf{X}_s \right|^n \mathbf{n}^n,$$

$$\mathbf{F}^n = \mathbf{F}_\sigma^n + \mathbf{F}_b^n$$

2. Solve the Navier-Stokes

$$(3\mathbf{u}^* - 4\mathbf{u}^n + \mathbf{u}^{n-1})/(2\Delta t) + \left(2(\mathbf{u}^n \cdot \nabla_h)\mathbf{u}^n - (\mathbf{u}^{n-1} \cdot \nabla_h)\mathbf{u}^{n-1}\right)$$

$$= -\nabla_h p^n + \mu \widetilde{\Delta}_h \mathbf{u}^* + \sum_s \mathbf{F}^n(s) \delta_h(\mathbf{x} - \mathbf{X}^n(s)) \Delta s$$

$$\Delta_h \phi = 3/(2\Delta t) \nabla_h \cdot \mathbf{u}^*, \quad \partial\phi/\partial\mathbf{n} = 0 \text{ on } \partial\Omega$$

$$\mathbf{u}^{n+1} = \mathbf{u}^* - \frac{2}{3}\Delta t \nabla_h \phi, \quad \nabla_h p^{n+1} = \nabla_h \phi + \nabla_h p^n - \frac{2}{3}\Delta t \mu \widetilde{\Delta}_h (\nabla_h \phi)$$

3. Update the new position

$$\mathbf{X}_k^{n+1} = \mathbf{X}_k^n + \Delta t \sum_{\mathbf{x}} \mathbf{u}^{n+1} \delta_h(\mathbf{x} - \mathbf{X}^n(s)) h^2$$

Axis-symmetric case, Hu, Kim & Lai, JCP 2014

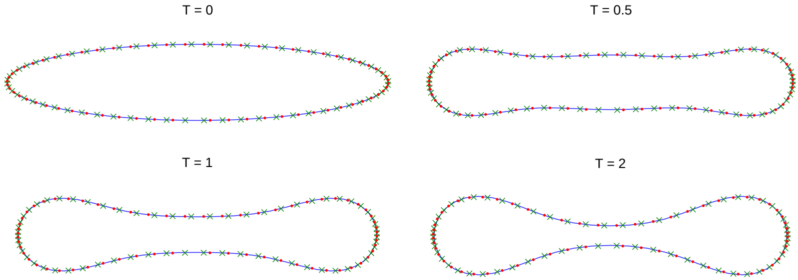

Figure: Freely suspended vesicles with different penalty number σ_0. Blue solid line: $\sigma_0 = 2 \times 10^3$; green marker "×": $\sigma_0 = 2 \times 10^4$; red marker "·": $\sigma_0 = 2 \times 10^5$.

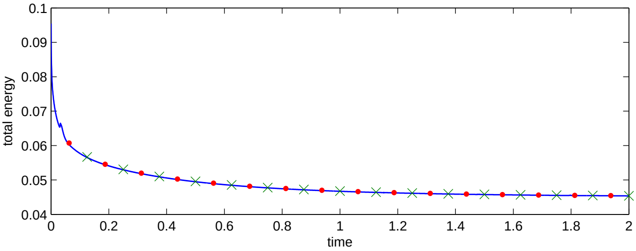

Figure: The corresponding evolution of total energy. Blue solid line: $\sigma_0 = 2 \times 10^3$; green marker "$\times$": $\sigma_0 = 2 \times 10^4$; red marker "$\cdot$": $\sigma_0 = 2 \times 10^5$

σ_0	$\| R \lvert \mathbf{X}_s \rvert - R^0 \lvert \mathbf{X}_s \rvert^0 \|_\infty$	$\lvert A_h - A_0 \rvert / A_0$	$\lvert V_h - V_0 \rvert / V_0$
2×10^3	2.988E-04	2.431E-03	9.391E-04
2×10^4	6.551E-05	2.060E-04	2.865E-04
2×10^5	2.903E-05	2.105E-05	2.657E-04

Table: The errors of the area dilating factor, the total surface area, and the volume.

Convergence test

- Initial shape $\mathbf{X}(s) = (0.5\cos s, 0.15\sin s)$ in quiescent flow
- Computational domain Ω is chosen as $[0,1]\times[-0.5,0.5]$
- Take $c_b = 2\times 10^{-2}$ and $\sigma_0 = 2\times 10^4$. $T = 0.5$, $m = n = 512$ as a reference numerical solution

	$m = 64$	$m = 128$	rate	$m = 256$	rate
$\lvert A_h - A_0\rvert/A_0$	4.032E-04	2.024E-04	0.99	1.009E-04	1.00
$\lvert V_h - V_0\rvert/V_0$	6.434E-04	1.505E-04	2.10	3.170E-05	2.25
$\lVert\mathbf{X}_h - \mathbf{X}_{\mathrm{ref}}\rVert_\infty$	1.689E-03	4.625E-04	1.87	9.937E-05	2.22
$\lVert u_h - u_{\mathrm{ref}}\rVert_\infty$	2.363E-03	1.162E-03	1.02	5.321E-04	1.13

Table: The mesh refinement results for the perimeter of the surface area A_h, the enclose volume V_h, the interface configuration $\mathbf{X}_h$, and the velocity u_h.

Numerical experiments

A freely suspended vesicle

- Computational domain $\Omega = [0, 0.5] \times [-1, 1]$
- Quiescent flow $\mathbf{u} = \mathbf{0}$
- Bending coefficient $c_b = 5 \times 10^{-2}$

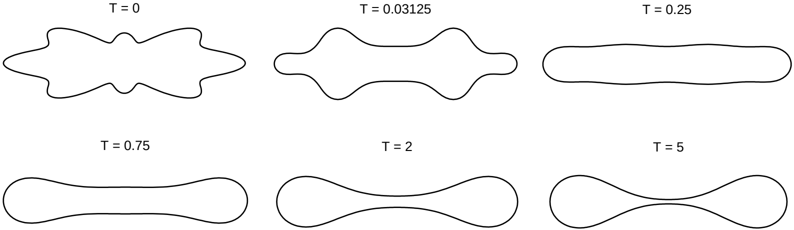

Figure: Snapshots of a freely suspended vesicle in quicient flow.

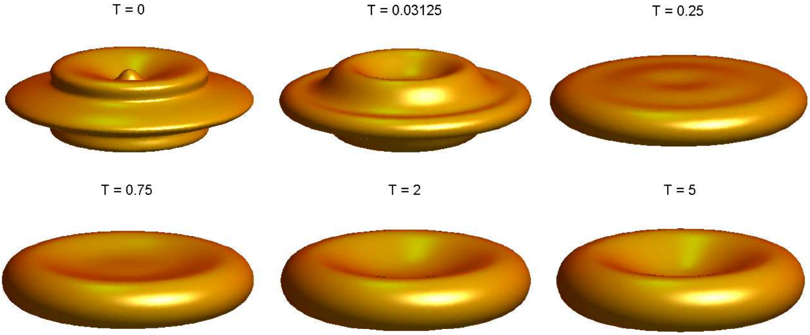

Figure: The coressponding result in 3D view.

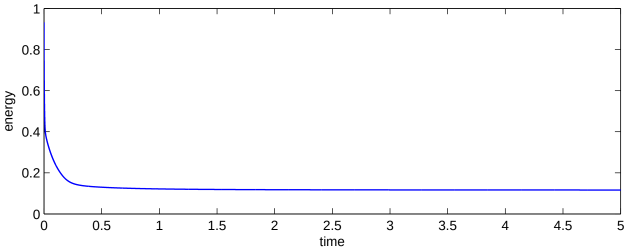

Figure: The membrane energy evolution of the freely suspended vesicle.

Gravitational effect

- The additional interfacial force $\mathbf{F}_g$ is considered due to gravity $\mathbf{g}$ is given by

$$\mathbf{F}_g = (\rho^{\text{in}} - \rho^{\text{out}})(\mathbf{g} \cdot \mathbf{X}) \left|\mathbf{X}_s\right| \mathbf{n}$$

- Computational domain Ω_h is chosen as $[0, 1] \times [-2, 2]$

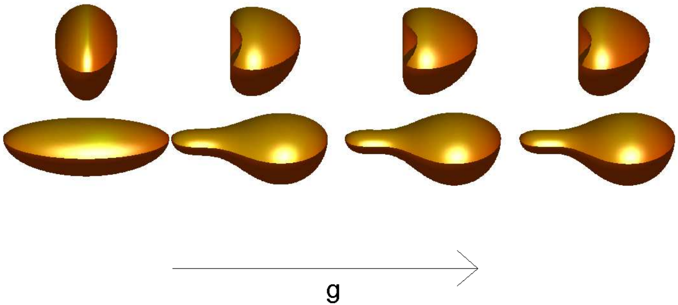

Figure: Top: oblate shape ⇒ parachute-like; Bottom: prolate shape ⇒ pear-like shape. Consistent with experiments.

Full 3D case: Seol, Hu, Kim & Lai JCP 2016

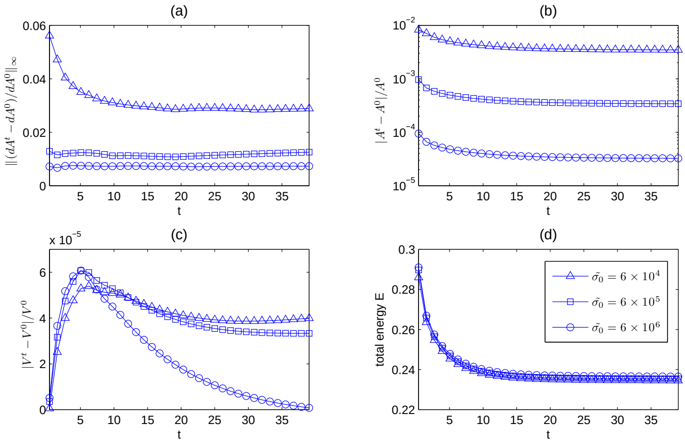

Figure: The comparison for three different stiffness parameters: $\tilde{\sigma_0} = 6 \times 10^4(\triangle)$, $6 \times 10^5(\square)$, and $6 \times 10^6(\bigcirc)$. (a) the maximum relative error of the local surface area; (b) the relative error of the global surface area; (c) the relative error of the global volume; (d) the total energy.

Vesicle under shear flow

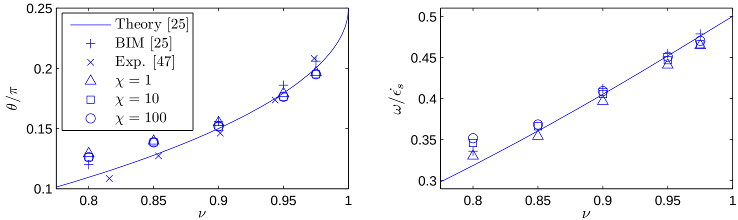

Figure: The plot of the inclination angle (left) and the scaled mean angular velocity (right) as functions of reduced volume ν for different dimensionless shear rate χ.

- The frequency ω can be computed using $\omega = \frac{1}{N_v}\sum_{i=1}^{N_v} \frac{|\mathbf{r}\times\mathbf{v}|}{|\mathbf{r}|^2}$, where $\mathbf{r}$ and $\mathbf{v}$ are the position and velocity of the vertices projected on the xz-plane, respectively.

Viscoelastic effects on vesicle dynamics, Seol, Tseng, Kim, & Lai 2018

- Motivation: vesicles mimic the red blood cells (RBCs), and the blood containing RBCs and plasma exhibits non-Newtonian properties [S. Chien 1970, G.B. Thurston 1973,1979]
- Newtonian vs. non-Newtonian fluid: the relation between the shear stress and shear rate is linear (Newtonian); otherwise, it is non-Newtonian
- Viscoelasticity: non-Newtonian fluid exhibits both viscous and elastic characteristics when is undergoing deformation
- Non-Newtonian fluid examples: ketchup, toothpaste, paint, blood, and shampoo etc.
- Oldroyd-B model is used in the present work

Newtonian vesicle in non-Newtonian fluid (N/O)

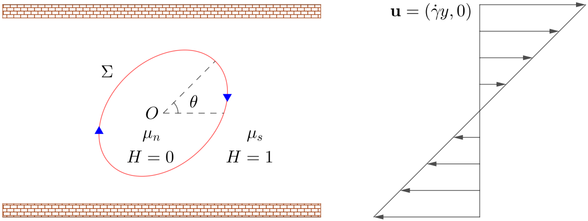

Figure: The vesicle is filled with a Newtonian fluid while the suspended fluid is an Oldryod-B fluid (a mixture of polymer and Newtonian solvent), denoted by N/O fluid.

For a vesicle under shear flow, two types of motion have been well investigated

- tank-treading (TT) motion
- tumbling (TB) motion

Governing equations of fluid vesicle system

$$\rho\left(\frac{\partial \mathbf{u}}{\partial t}+(\mathbf{u}\cdot\nabla)\mathbf{u}\right)=-\nabla p+\nabla\cdot[((1-H)\mu_n+H\mu_s)\,\mathbb{D}(\mathbf{u})+H\sigma]+\mathbf{f}\quad \text{in } \Omega,$$

$$\nabla\cdot\mathbf{u}=0\quad \text{in } \Omega,$$

$$\mathbf{f}(\mathbf{x},t)=\int_\Sigma(\mathbf{F}_\gamma+\mathbf{F}_b)(\alpha,t)\,\delta(\mathbf{x}-\mathbf{X}(\alpha,t))|\mathbf{X}_\alpha|\,\mathrm{d}\alpha\quad \text{in } \Omega,$$

$$\frac{\partial \mathbf{X}}{\partial t}(\alpha,t)=\mathbf{U}(\alpha,t)=\int_\Omega \mathbf{u}(\mathbf{x},t)\,\delta(\mathbf{x}-\mathbf{X}(\alpha,t))\,\Delta x\quad \text{on } \Sigma,$$

$$\gamma(\alpha,t)=\gamma_0\left(\frac{|\mathbf{X}_\alpha(\alpha,t)|}{|\mathbf{X}_\alpha(\alpha,0)|}-1\right)\quad \text{on } \Sigma,$$

$$\mathbf{F}_\gamma(\alpha,t)=\frac{1}{|\mathbf{X}_\alpha|}\frac{\partial(\gamma\tau)}{\partial\alpha},\qquad \mathbf{F}_b(\alpha,t)=c_b\left(\kappa_{ss}+\frac{\kappa^3}{2}\right)\mathbf{n}\quad \text{on } \Sigma,$$

Governing equations of polymer stress (Oldroyd-B model)

For a symmetric polymer stress defined by

$$\sigma = \begin{bmatrix} \sigma^a & \sigma^b \\ \sigma^b & \sigma^c \end{bmatrix},$$

its governing equation is

$$\xi \overset{\triangledown}{\sigma} + \sigma = \mu_p \, \mathbb{D}(\mathbf{u}) \quad \text{in } \Omega,$$

where

$$\overset{\triangledown}{\sigma} = \frac{\partial \sigma}{\partial t} + \mathbf{u} \cdot \nabla \sigma - \left(\nabla \mathbf{u} \sigma + \sigma (\nabla \mathbf{u})^T \right),$$

$$\mathbb{D}(\mathbf{u}) = \nabla \mathbf{u} + (\nabla \mathbf{u})^T.$$

ξ is the polymer relaxation time, $\overset{\triangledown}{\sigma}$ is the upper convected time derivative of σ, and $\mathbb{D}(\mathbf{u})$ is the rate of deformation tensor. For the Eulerian grid point $\mathbf{x} = (x, y)$, H is the indicator (or Heaviside step) function defined by,

$$H(\mathbf{x}) = \begin{cases} 1 & \text{if } \mathbf{x} \text{ is in Oldroyd-B fluid} \\ 0 & \text{if } \mathbf{x} \text{ is in Newtonian fluid.} \end{cases}$$

Governing equations in dimensionless form

$$\mathrm{Re}\left(\frac{\partial \mathbf{u}}{\partial t} + (\mathbf{u}\cdot\nabla)\mathbf{u}\right) = -\nabla p + \nabla\cdot\left[\left((1-H)\lambda + H\right)\mathbb{D}(\mathbf{u}) + H\sigma\right] + \mathbf{f} \quad \text{in } \boldsymbol{\Omega},$$

$$\nabla\cdot\mathbf{u} = 0 \quad \text{in } \Omega,$$

$$\mathbf{f}(\mathbf{x},t) = \int_\Sigma \left(\mathbf{F}_\gamma + \mathbf{F}_b\right)(\alpha,t)\,\delta(\mathbf{x}-\mathbf{X}(\alpha,t))|\mathbf{X}_\alpha|\,\mathrm{d}\alpha \quad \text{in } \Omega,$$

$$\frac{\partial \mathbf{X}}{\partial t}(\alpha,t) = \mathbf{U}(\alpha,t) = \int_\Omega \mathbf{u}(\mathbf{x},t)\,\delta(\mathbf{x}-\mathbf{X}(\alpha,t))\,d\mathbf{x} \quad \text{on } \Sigma,$$

$$\gamma(\alpha,t) = \gamma_0\left(\frac{|\mathbf{X}_\alpha(\alpha,t)|}{|\mathbf{X}_\alpha(\alpha,0)|} - 1\right) \quad \text{on } \Sigma,$$

$$\mathbf{F}_\gamma(\alpha,t) = \frac{1}{|\mathbf{X}_\alpha|}\frac{\partial(\gamma\tau)}{\partial\alpha}, \quad \mathbf{F}_b(\alpha,t) = \frac{1}{\mathrm{Ca}}\left(\kappa_{ss} + \frac{\kappa^3}{2}\right)\mathbf{n} \quad \text{on } \Sigma,$$

$$\mathrm{Wi}\,\overset{\triangledown}{\sigma} + \sigma = \beta\,\mathbb{D}\mathbf{u} \quad \text{in } \Omega,$$

where

$$\mathrm{Re} = \frac{\rho R^2}{\mu_s t_c}, \quad \mathrm{Ca} = \frac{\mu_s R^3}{c_b t_c}, \quad \mathrm{Wi} = \frac{\xi}{t_c}, \quad \lambda = \frac{\mu_n}{\mu_s}, \quad \beta = \frac{\mu_p}{\mu_s}.$$

For the 1D vesicle boundary $\mathbf{X}(\alpha, t) = (X(\alpha, t), Y(\alpha, t))$, the operators are

- $\nabla_s \sigma = \dfrac{\tau}{|\mathbf{X}_\alpha|} \dfrac{\partial \sigma}{\partial \alpha}$
- $\nabla_s \cdot \mathbf{U} = \dfrac{\tau}{|\mathbf{X}_\alpha|} \cdot \dfrac{\partial \mathbf{U}}{\partial \alpha}$
- $\kappa_{ss} = \dfrac{1}{|\mathbf{X}_\alpha|} \dfrac{\partial}{\partial \alpha} \left(\dfrac{1}{|\mathbf{X}_\alpha|} \dfrac{\partial \kappa}{\partial \alpha} \right) = \dfrac{-\mathbf{X}_\alpha \cdot \mathbf{X}_{\alpha\alpha}}{|\mathbf{X}_\alpha|^4} \dfrac{\partial \kappa}{\partial \alpha} + \dfrac{1}{|\mathbf{X}_\alpha|^2} \dfrac{\partial^2 \kappa}{\partial \alpha^2}$
- The unit tangent vector $\tau = (\tau_1, \tau_2) = \mathbf{X}_\alpha / |\mathbf{X}_\alpha|$
- The unit normal vector $\mathbf{n} = (\tau_2, -\tau_1)$
- The signed curvature $\kappa = \dfrac{X_\alpha Y_{\alpha\alpha} - Y_\alpha X_{\alpha\alpha}}{(X_\alpha^2 + Y_\alpha^2)^{3/2}}$

Discretization of Eulerian and Lagrangian variables

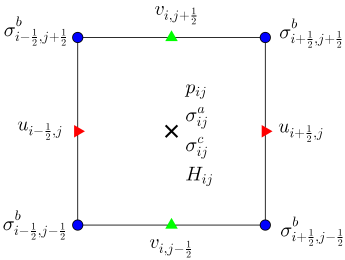

Figure: Fluid variables on a staggered MAC grid in 2D. Chrispell et. al. 2011

- For a periodic interface $\mathbf{X}$, we use a Fourier representation to discretize it as

$$\mathbf{X}(\alpha, t) = \sum_{k=-N/2}^{N/2-1} \widehat{\mathbf{X}}(k,t)e^{ik\alpha}.$$

Numerical algorithm

We march the Lagrangian markers $\mathbf{X}^n = \mathbf{X}(n\Delta t)$ from time level n to obtain $\mathbf{X}^{n+1} = \mathbf{X}(n\Delta t + \Delta t)$ at time level $n+1$ with Δt the time step size. The polymer stress σ^n, the fluid velocity $\mathbf{u}^n$, the pressure p^n, and the Lagrangian markers $\mathbf{X}^n$ are all given in advance, and from these variables we update σ^{n+1}, $\mathbf{u}^{n+1}$, p^{n+1}, and $\mathbf{X}^{n+1}$.

1. Compute the vesicle boundary forces.

   At the Lagrangian markers $\mathbf{X}_\ell^n$,

   we calculate the spring-like tension $\gamma(\mathbf{X}_\ell^n) = \gamma_0 \left(\frac{|(\mathbf{X}_\alpha)_\ell^n|}{|(\mathbf{X}_\alpha)_\ell^0|} - 1 \right)$,

   and then incorporate those to compute the interfacial forces

$$\mathbf{F}_\gamma(\mathbf{X}_\ell^n) = \frac{1}{|(\mathbf{X}_\alpha)_\ell^n|} \left(\frac{\partial \gamma \tau}{\partial \alpha} \right)_\ell^n,$$

$$\mathbf{F}_b(\mathbf{X}_\ell^n) = \frac{1}{\mathrm{Ca}} \left(-\frac{(\mathbf{X}_\alpha)_\ell^n \cdot (\mathbf{X}_{\alpha\alpha})_\ell^n \, (\kappa_\alpha)_\ell^n}{|(\mathbf{X}_\alpha)_\ell^n|^4} + \frac{(\kappa_{\alpha\alpha})_\ell^n}{|(\mathbf{X}_\alpha)_\ell^n|^2} + \frac{(\kappa_\ell^n)^3}{2} \right) \mathbf{n}_\ell^n.$$

2. Distribute the tension and bending forces acting on Lagrangian markers into the Eulerian grid by using the smoothed Dirac delta function δ_h as

$$\mathbf{f}^n(\mathbf{x}) = \sum_{\ell=0}^{N-1} (\mathbf{F}_\gamma(\mathbf{X}_\ell^n) + \mathbf{F}_b(\mathbf{X}_\ell^n))\delta_h(\mathbf{x} - \mathbf{X}_\ell^n)\, \mathrm{d}s(\mathbf{X}_\ell^n),$$

where the curve length element is obtained by $\mathrm{d}s(\mathbf{X}_\ell^n) = |(\mathbf{X}_\alpha)_\ell^n|\Delta\alpha$.

For $\delta_h(\mathbf{x}) = \frac{1}{h^2}\phi\left(\frac{x}{h}\right)\phi\left(\frac{y}{h}\right)$,

we employ 6-point supported C^3 function ϕ

developed in [Bao et.al, JCP'16].

3. Solve the Navier-Stokes

$$\begin{aligned}
&\mathrm{Re}\left(\frac{3\mathbf{u}^{*}-4\mathbf{u}^{n}+\mathbf{u}^{n-1}}{2\Delta t}+2\left(\mathbf{u}^{n}\cdot\nabla_{h}\right)\mathbf{u}^{n}-\left(\mathbf{u}^{n-1}\cdot\nabla_{h}\right)\mathbf{u}^{n-1}\right)\\
&=-\nabla_{h}p^{n}+\lambda\Delta_{h}\mathbf{u}^{*}+\nabla_{h}\cdot\left[(1-\lambda)H\left(\nabla_{h}\mathbf{u}^{n}+(\nabla_{h}\mathbf{u}^{n})^{T}\right)\right]\\
&\quad+\nabla_{h}\cdot(H\sigma^{n})+\mathbf{f}^{n},\\
&\Delta_{h}p^{\star}=\frac{3\,\mathrm{Re}}{2\Delta t}\nabla_{h}\cdot\mathbf{u}^{*},\quad \frac{\partial p^{\star}}{\partial\mathbf{n}}=0 \text{ on } \partial\Omega,\quad \mathbf{u}^{*}=\mathbf{u}^{n+1} \text{ on } \partial\Omega,\\
&\mathbf{u}^{n+1}=\mathbf{u}^{*}-\frac{2\Delta t}{3\,\mathrm{Re}}\nabla_{h}p^{\star},\nabla_{h}p^{n+1}=\nabla_{h}p^{\star}+\nabla_{h}p^{n}-\frac{2\lambda\Delta t}{3\,\mathrm{Re}}\Delta_{h}(\nabla_{h}p^{\star}).
\end{aligned}$$

4. Update the new position

$$\mathbf{X}_{k}^{n+1}=\mathbf{X}_{k}^{n}+\Delta t\sum_{\mathbf{x}}\mathbf{u}^{n+1}(\mathbf{x})\delta_{h}(\mathbf{x}-\mathbf{X}_{k}^{n})h^{2}$$

5. Solve the polymer stress equation

$$\frac{\partial \sigma}{\partial t} = \mathbb{F}(\sigma, \mathbf{u}),$$

where

$$\mathbb{F}(\sigma, \mathbf{u}) = -\mathbf{u} \cdot \nabla \sigma + \left(\nabla \mathbf{u} \sigma + \sigma (\nabla \mathbf{u})^T \right) - \frac{\sigma}{\mathrm{Wi}} + \frac{\beta}{\mathrm{Wi}} \left(\nabla \mathbf{u} + (\nabla \mathbf{u})^T \right).$$

To find σ^{n+1}, we use the second-order Runge-Kutta (RK2) method with zero-Neumann boundary condition at Dirichlet boundary of fluid velocity. Two intermediate variables σ_1 and σ_2 are defined by

$$\sigma_1 = \sigma^n + \Delta t \, \mathbb{F}(\sigma^n, \mathbf{u}^n),$$

$$\sigma_2 = \sigma_1 + \Delta t \, \mathbb{F}(\sigma_1, \mathbf{u}^{n+1}),$$

the updated extra stress is obtained from

$$\sigma^{n+1} = (\sigma^n + \sigma_2)/2.$$

Numerical accuracy test for Oldroyd-B solver

We test a single-phase Oldroyd-B fluid in a computational domain $[0, 2\pi] \times [\pi/2, 5\pi/2]$.

$$\mathrm{Re}\left(\frac{\partial \mathbf{u}}{\partial t} + (\mathbf{u}\cdot\nabla)\mathbf{u}\right) = -\nabla p + \Delta\mathbf{u} + \nabla\cdot\sigma \quad \text{in } \Omega,$$

$$\nabla\cdot\mathbf{u} = 0 \quad \text{in } \Omega,$$

$$\mathrm{Wi}\,\overset{\triangledown}{\sigma} + \sigma = \beta\,\mathbb{D}\mathbf{u} + \phi \quad \text{in } \Omega,$$

where

$$\begin{aligned}
\phi &= \mathrm{Wi}\,\beta\left[\begin{array}{cc} \phi^a & \phi^b \\ \phi^b & \phi^c \end{array}\right], \\
\phi^a &= -2G^{'}\sin x\sin y - 2G^2\cos^2 x\sin^2 y + 2G^2\sin^2 x\cos^2 y \\
&\quad -4G^2\sin^2 x\sin^2 y, \\
\phi^b &= -4G^2\sin x\cos x\sin y\cos y, \\
\phi^c &= 2G^{'}\sin x\sin y + 2G^2\cos^2 x\sin^2 y - 2G^2\sin^2 x\cos^2 y \\
&\quad -4G^2\sin^2 x\sin^2 y, \\
G(t) &= e^{-2(1+\beta)t/Re}.
\end{aligned}$$

The exact analytical solution of the above equations is

$$\mathbf{u}_e = (G\cos x \sin y, -G \sin x \cos y),$$

$$p_e = -\frac{\mathrm{Re}}{4}(\cos 2x + \cos 2y)G^2,$$

$$\sigma_e = \beta\,\mathbb{D}\mathbf{u} = \beta \begin{bmatrix} -2G\sin x \sin y & 0 \\ 0 & 2G \sin x \sin y \end{bmatrix}.$$

- $\mathrm{Re} = \mathrm{Wi} = \beta = 1$ and $\Delta t = h/8$, where the h is the Eulerian meshwidth defined by $h = 2\pi/M$ with grid size M.
- Convergence rate is obtained by

$$\mathrm{Rate} = \log_2(\|u_M - u_e\|_\infty / \|u_{2M} - u_e\|_\infty),$$

M	$\|u_M - u_e\|_\infty$	Rate	$\|v_M - v_e\|_\infty$	Rate	$\|p_M - p_e\|_\infty$	Rate
$(t = 0.6)$						
64	1.287E-02	-	1.173E-02	-	4.270E-02	-
128	6.291E-03	1.03	5.735E-03	1.03	2.181E-02	0.96
256	3.108E-03	1.01	2.833E-03	1.01	1.100E-02	0.98
512	1.544E-03	1.00	1.408E-03	1.00	5.522E-03	0.99
$(t = 1.2)$						
64	9.512E-03	-	8.290E-03	-	3.775E-02	-
128	4.697E-03	1.01	4.091E-03	1.01	1.935E-02	0.96
256	2.334E-03	1.00	2.033E-03	1.00	9.780E-03	0.98
512	1.163E-03	1.00	1.013E-03	1.00	4.914E-03	0.99

M	$\|\sigma^a_M - \sigma^a_e\|_\infty$	Rate	$\|\sigma^b_M - \sigma^b_e\|_\infty$	Rate	$\|\sigma^c_M - \sigma^c_e\|_\infty$	Rate
$(t = 0.6)$						
64	8.391E-02	-	1.035E-02	-	8.508E-02	-
128	4.697E-02	0.99	5.286E-03	0.96	4.234E-02	1.00
256	2.099E-02	1.00	2.661E-03	0.99	2.108E-02	1.00
512	1.049E-02	1.00	1.334E-03	0.99	1.052E-02	1.00
$(t = 1.2)$						
64	4.583E-02	-	1.765E-02	-	4.660E-02	-
128	2.329E-02	0.97	8.937E-03	0.98	2.351E-02	0.98
256	1.173E-02	0.98	4.486E-03	0.99	1.179E-02	0.99
512	5.887E-03	0.99	2.247E-03	0.99	5.903E-03	0.99

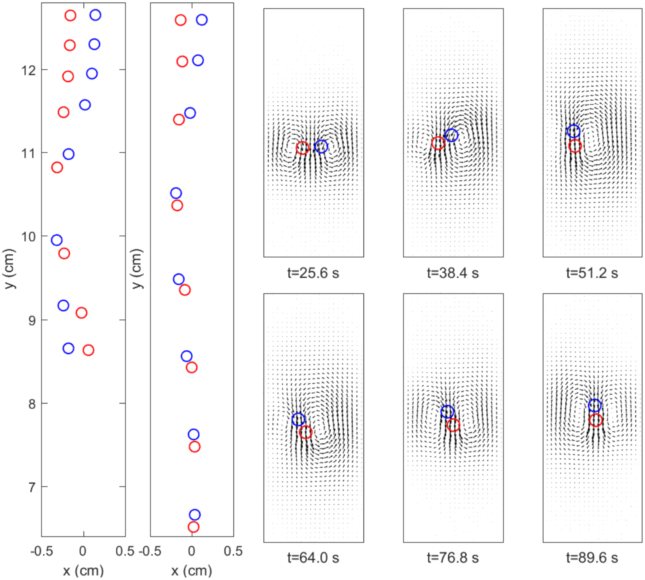

Figure: Two particles sedimentation. Left (Newtonian); right (Oldroyd-B); Kim, Lai, Seol, J. Non-Newtonian Fluid Mech., 2018

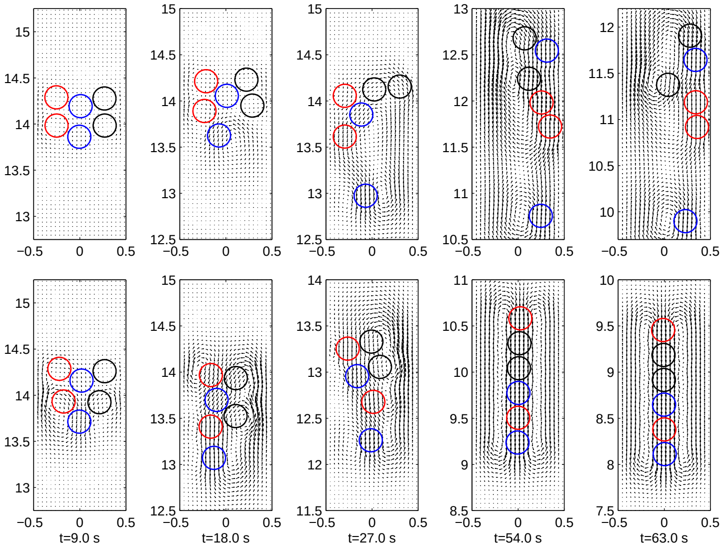

Figure: Six particles sedimentation. Top (Newtonian); bottom (Oldroyd-B); Kim, Lai, Seol, J. Non-Newtonian Fluid Mech., 2018

Numerical results

Goal

- Exploring the effects of viscoelasticity on vesicle dynamics under shear flow, mainly on the Newtonian vesicle suspended in Oldroyd-B fluid, denoted by N/O
- Parameter study
  - Weissenberg number Wi
  - viscosity contrast β between polymer and Newtonian solvent
  - Reynolds number Re
  - viscosity contrast λ between inner and outer fluids
  - reduced area $\nu = 4\pi A/L^2$: the area ratio between the vesicle and the circle with same perimeter

Numerical parameters

Unless otherwise stated, we use

- $\mathrm{Re} = 10^{-3}$, $\beta = 1$, $\mathrm{Ca} = 1$, $A = \pi$, $\Delta t = h^2/4$
- $\gamma_0 = 5 \times 10^3$, meshwidth $h = 16/512$, $[-8, 8]^2$ with grid size 512^2
- Number of Lagrangian markers $N = 1024$, simulation up to $t = 50$

Comparison of N/N and N/O fluids

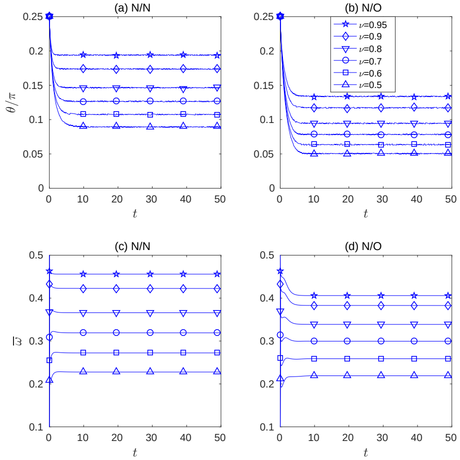

Figure: For various ν and fixed $\mathrm{Ca} = 1$, the inclination angle θ/π in (a,b); The average TT frequency ϖ in (c,d).

Weissenberg number effect

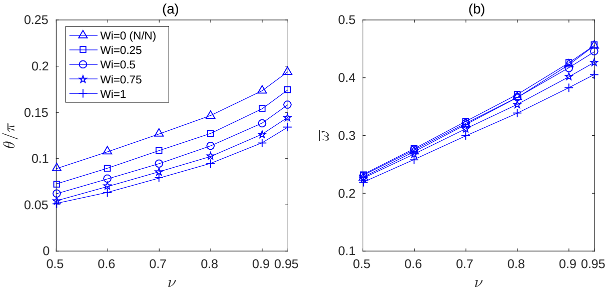

Figure: For various Wi and fixed Ca = 1, (a) the inclination angle θ/π and (b) the average TT frequency $\overline{\omega}$ both in terms of ν.

$$\overline{\omega}(t) = 2\pi \Big/ \int_{\Sigma(t)} \frac{|\mathbf{X}_\alpha|}{|\mathbf{U}\cdot\tau|}\, \mathrm{d}\alpha,$$

Viscosity ratio between polymer and Newtonian solvent effect

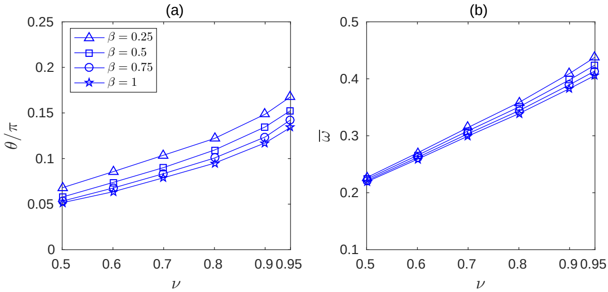

Figure: For various β and fixed $\mathrm{Ca} = 1$, (a) the inclination angle θ/π and (b) the average TT frequency $\overline{\omega}$ both in terms of ν.

Reynolds number effect

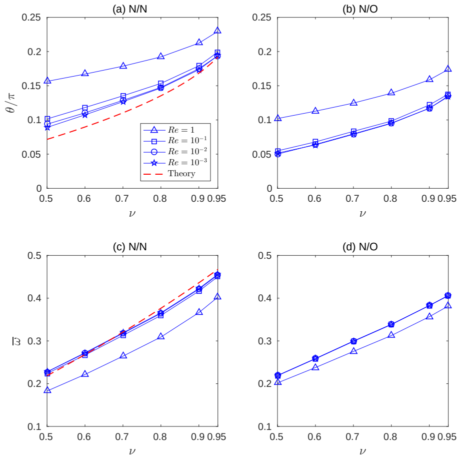

Figure: For various Re and fixed Ca = 1, the inclination angle θ/π in (a,b); The average TT frequency $\overline{\omega}$ in (c,d).

Viscosity contrast between inner and outer fluids

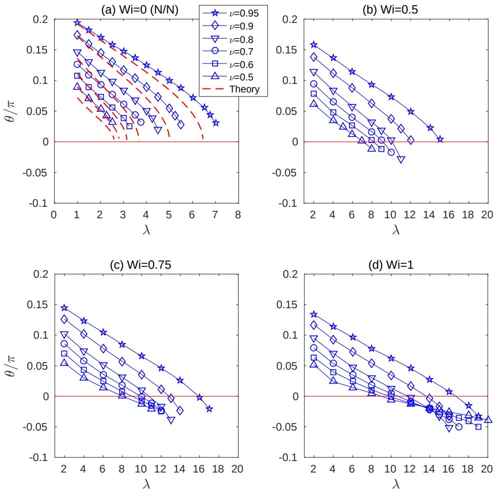

Figure: For various Wi and fixed Ca $= 1$, the inclination angle θ/π in terms of the viscosity contrast λ.

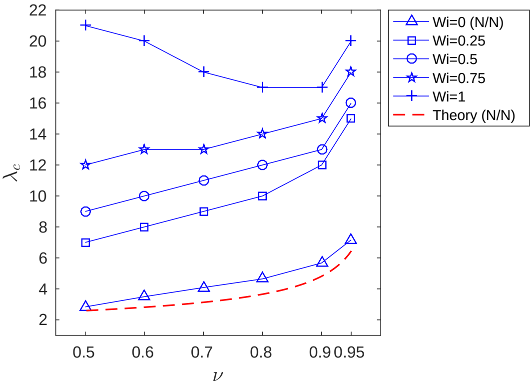

Figure: For various Wi and fixed Ca $= 1$, the critical viscosity contrast λ_c in terms of the reduced area ν.

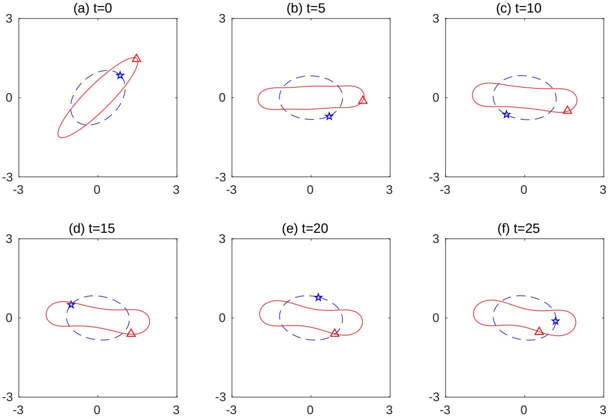

Figure: Snapshots of TT vesicles with $\nu = 0.5, \lambda = 20$ (red solid line) and $\nu = 0.95, \lambda = 19$ (blue dashed line) suspended in N/O fluid with fixed $\mathrm{Re} = 10^{-3}, \mathrm{Ca} = 1$, and $\mathrm{Wi} = 1$.

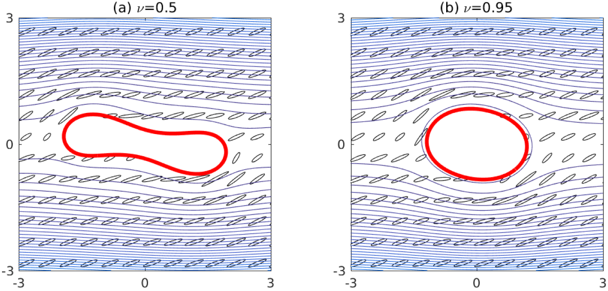

Figure: In N/O fluid with fixed $\mathrm{Re} = 10^{-3}, \mathrm{Ca} = 1$, and $\mathrm{Wi} = 1$, streamlines and stress-ellipses at time $t = 50$ for vesicles with $\nu = 0.5, \lambda = 20$ in (a) and $\nu = 0.95, \lambda = 19$ in (b).

Different Reynolds number in unmatched viscosity fluid

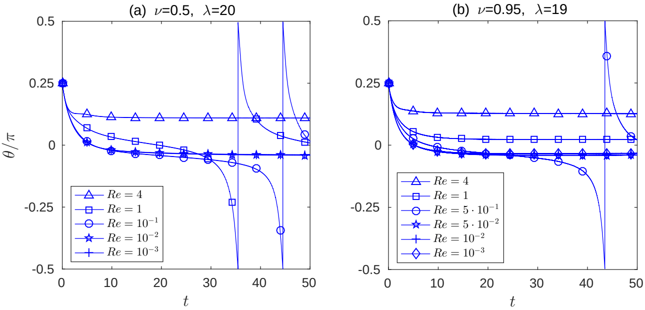

Figure: In unmatched viscosity N/O fluid with fixed $\mathrm{Ca} = 1$ and $\mathrm{Wi} = 1$, the time evolution of inclination angle for a vesicle with $\nu = 0.5, \lambda = 20$ in (a) and $\nu = 0.95, \lambda = 19$ in (b).

Conclusion

- In matched viscosity N/O fluid, the vesice inclination angle in TT regime decreases with increasing Weissenberg number
- In unmatched viscosity case, the angle decreases even more as the viscosity contrast increases.

Most surprisingly, the negative inclination angle was found in TT regime, indicating that the viscoelasticity of suspending fluid tends to lag the TU motion.

- A vesicle tank-treads at negative inclination angle at small Reynolds number, then abruptly tumbles at slightly higher Reynolds number, and returns back to tank-tread at positive inclination angle at even higher Reynolds number. We attribute this behavior to the interplay between the viscoelasticity and the inertia.